Ultrasound in Med. & Biol., Vol. 44, No. 1, pp. 168–176, 2018

0301-5629/$ - see front matter

https://doi.org/10.1016/j.ultrasmedbio.2017.09.002

● *Original Contribution*

AUTOMATIC MEASUREMENTS OF MITRAL ANNULAR PLANE SYSTOLIC EXCURSION AND VELOCITIES TO DETECT LEFT VENTRICULAR DYSFUNCTION

Jahn Frederik Grue,* Sigurd Storve,* Håvard Dalen,*†‡ Øyvind Salvesen,§ Ole Christian Mjølstad,*† Stein O. Samstad,*† Hans Torp,* and Bjørn Olav Haugen*

* Department of Circulation and Medical Imaging, Faculty of Medicine and Health Sciences, NTNU, Norwegian University of Science and Technology, Trondheim, Norway; † Department of Cardiology, St. Olavs hospital, Trondheim University Hospital, Trondheim, Norway; ‡ Department of Internal Medicine, Levanger Hospital, Nord-Trøndelag Hospital Trust, Levanger, Norway; and § Department of Public Health and Nursing, Faculty of Medicine and Health Sciences, NTNU, Norwegian University of Science and Technology, Trondheim, Norway

(*Received* 24 *March* 2017; *revised* 21 *July* 2017; *in final form* 1 *September* 2017)

Abstract—The purpose of the study described here was to evaluate an automatic algorithm for detection of left ventricular dysfunction, based on measurements of mitral annular motion indices from color tissue Doppler apical four-chamber recordings. Two hundred twenty-one patients, among whom 49 had systolic and 11 had diastolic dysfunction, were included. Echocardiographic evaluation by cardiologists was the reference. Twenty patients were also examined by medical students. The ability of the indices to detect systolic and diastolic dysfunction were compared in receiver operating characteristic analyses, and the agreement between automatic and reference measurements was evaluated. Mitral annular plane systolic excursion ≤10 mm detected left ventricular dysfunction with 82% specificity, 76% specificity, 56% positive predictive value and 92% negative predictive value. The automatic measurements acquired from expert recordings better agreed better with the reference than those acquired from student recordings. We conclude that automatic measurements of systolic mitral annular motion indices can be helpful in detection of left ventricular dysfunction. (E-mail: Bjorn.o.haugen@ntnu.no) **© 2018 The Author(s). Published by Elsevier Inc. on behalf of World Federation for Ultrasound in Medicine & Biology. This is an open access article under the CC BY-NC-ND license (http://creativecommons.org/licenses/by-nc-nd/4.0/).**

Key Words: **Atrioventricular, Displacement, Heart failure, HFpEF (heart failure with preserved ejection fraction), HFrEF (heart failure with reduced ejection fraction), Tissue Doppler.**

INTRODUCTION

Between 1% and 2% of the adult population in the Western world have heart failure, and 10% of people aged ≥70 y are affected (Ponikowski et al. 2016). Taking care of all these patients is a huge task for the specialized health care service. The complexity of echocardiography limits its usefulness for inexperienced users (Atherton 2010). Automated measurements and interpretations of findings may improve the use of echocardiography among non-expert users.

Heart failure is most often due to a variable degree of systolic and/or diastolic left ventricular (LV) dysfunction. Several echocardiographic parameters including LV ejection fraction (EF), Doppler-based indices and sizes of cardiac chambers are commonly combined to assess LV function (Ponikowski et al. 2016). This is a comprehensive task reserved for experts and requires the use of multiple echocardiographic modalities not feasible for incorporation into pocket-sized imaging devices (PSIDs). Therefore, simplified solutions are needed for automated detection of heart failure using PSIDs.

Left ventricular longitudinal function is reduced in patients with systolic and diastolic dysfunction, and can be quantified by measuring the mitral annular plane systolic excursion (MAPSE), peak systolic (S') and peak early (e') and late (a') diastolic velocity (Bruch et al. 2003; Garcia et al. 2006; Yip et al. 2002). All these parameters can be

Address correspondence to: Bjørn Olav Haugen, Department of Circulation and Medical Imaging, Faculty of Medicine and Health Sciences, Norwegian University of Science and Technology, Prinsesse Kristinas gate 3, 7030 Trondheim, Norway. E-mail: Bjorn.o.haugen@ntnu.no

Conflict of Interest: B.O.H., H.D. and O.C.M. held positions at MI Lab, a center of research-based innovation that was funded by the Research Council of Norway (Grant 219282) and industry. The Center had a total budget of 124 million NOK from 2007 to 2015. B.O.H. also holds a position at CIUS, a similar center of research-based innovation that is funded by the Research Council of Norway and industry from 2016 to 2022. S.S., H.D. and O.C.M. held positions in a user-driven Research-based innovation project called Smartscan.

measured despite low image quality from the easily obtainable apical four-chamber view (Hu et al. 2013; Kadappu and Thomas 2015).

We have developed an algorithm that automatically measures MAPSE, S', e' and a' from color tissue Doppler (CTD) recordings, with good agreement compared with reference measurements (Storve et al. 2016). This algorithm could be implemented on future PSIDs. The main aim of this study was to evaluate the ability of the automatic algorithm to detect systolic and/or diastolic LV dysfunction using experienced cardiologists' echocardiographic evaluations of LV function as the reference. In addition, we evaluated the agreement between automatic and reference measurements when the algorithm was run on recordings by both experts and novices.

METHODS

Patients

The study population consisted of inpatients and outpatients referred for echocardiographic examination at the Department of Cardiology, St. Olavs hospital, Trondheim University Hospital, Trondheim, Norway. Inclusion criteria were age ≥18 y and referral for echocardiographic evaluation at the hospital. Patients were excluded if the echocardiographic recordings could not be interpreted by the cardiologists because of poor image quality. Demographic characteristics and cardiovascular comorbidity were obtained from the hospital's patient charts and the echocardiographic archive. Written informed consent was obtained from all patients. The Regional Committee for Medical and Health Research Ethics and the Norwegian Social Science Data Service approved the study, which was conducted according to the Declaration of Helsinki.

Echocardiographic examinations

All reference echocardiographic examinations were performed by experienced cardiologists or experienced sonography technicians, using a commercially available Vivid E9 with an M5S-D cardiac transducer (bandwidth 1.5–4.6 MHz) or Vivid 7 with an M3S cardiac transducer (bandwidth 1.5–4.0 MHz) (both GE Vingmed Ultrasound, Horten, Norway). The sonographers' recordings and measurements were approved by a cardiologist. The patients were examined in the left lateral decubitus position. An additional experienced cardiologist contributed in the post-processing. The recordings were analyzed online or in EchoPAC SWO (Version 113, GE Vingmed Ultrasound).

Student examinations. Medical students from the Norwegian University of Science and Technology (NTNU, Trondheim, Norway) participated in the study. On the day of participation, the students were explained how to acquire an apical four-chamber view, with printed image examples of correct and wrong views. The images were kept by the students for help during scanning. The apical four-chamber view is provided in Figure 1.

Immediately after the reference examination, patients were transferred to another room in the same department for examination by a medical student. The students used a Vivid 7 scanner with an M3S cardiac

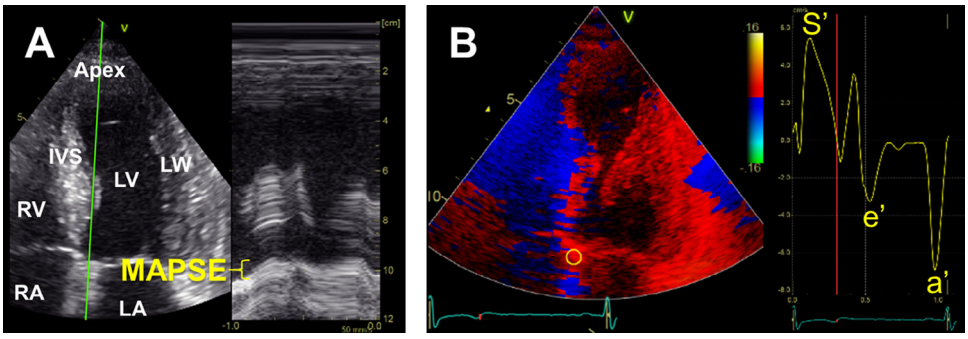

Fig. 1. The acquisition of reference measurements of mitral annular motion indices. (a) The mitral annular plane systolic excursion (MAPSE) is here measured using anatomic M-mode on a B-mode apical four-chamber recording, revealing the left (LV) and right (RV) ventricles, the left (LA) and right (RA) atria, the apex, the interventricular septum (IVS) and the left ventricular lateral wall (LW). The principle is the same as for regular M-mode measurements. A virtual M-mode scan line (*green*) is pointed at the edge of the mitral annulus (here at the septal side), as seen to the left. The echo signal along this 1-D line during one cardiac cycle is seen to the right. A caliper is used to measure the displacement of the annulus during systole, which corresponds to the distance within the *yellow, curly bracket*. The same process is repeated at the lateral side. Septal and lateral measurements from three consecutive heart cycles are averaged. (b) The mitral annular velocities are measured from apical four-chamber color tissue Doppler recordings. A stationary 5 × 5-mm sample volume is placed at the septal (*yellow ring*) and lateral (not marked here) sides of the annulus, as seen on the left. The septal tissue velocity curve from one cardiac cycle is seen on the right. The maximum positive velocity is the systolic peak velocity (S') and the maximum negative velocities are the early (e') and late (a') diastolic peak velocities. As for MAPSE, septal and lateral measurements from three consecutive heart cycles are averaged to calculate each index.

transducer, with tissue velocity imaging and gray-scale visualization activated. Image sector depth, width and gain settings were operated by the instructor. Students were offered a maximum of 15 min of scanning per patient, and each patient was examined by only one student. The students were asked to tell the instructor when they wanted the recording to be stored. The students were then told to keep the transducer in a steady position for 15 s, and the instructor saved the recording. If a student had time left and wanted to try again, the procedure was repeated. The students' last recordings were used in the analyses, as described under Mitral annular motion measurements.

Definition of left ventricular dysfunction

Guidelines of the European Association of Cardiovascular Imaging from 2009 and 2012 were followed to assess LV function (McMurray et al. 2012; Nagueh et al. 2009). Systolic dysfunction was defined as an EF <50%. Diastolic dysfunction was defined as an EF ≥50% in addition to several findings indicating increased LV filling pressure when present simultaneously. General criteria were septal e' <8 cm/s, lateral e' <10 cm/s, left atrial volume index (LAVI) >34 mL/m^2, early diastolic mitral inflow peak velocity (E) to late diastolic mitral inflow peak velocity (A) ratio (E/A) ≥2, E-Wave deceleration time <160 ms, isovolumic relaxation time (IVRT) <60 ms, pulmonary vein peak systolic flow velocity (S) to pulmonary vein peak diastolic flow velocity (D) ratio (S/D) < 1, tricuspid regurgitation peak velocity >3.4 m/s and the ratio between E and the average of septal and lateral e' (E/e') ≥13.

Basic echocardiographic measurements

Ejection fraction was measured with Simpson's biplane method. Mitral inflow velocities (E and A), E-wave deceleration time, pulmonary vein flow velocities (S and D), IVRT and tricuspid regurgitation peak velocity were measured from apical views using pulsed wave (PW) Doppler. e' was measured using PW tissue Doppler with the sample volume positioned in the basal part of the septal and lateral myocardium adjacent to the mitral annulus. Septal and lateral measurements were averaged, and E/e' was calculated. Left atrial volume was measured from apical views by the area–length method and divided by body surface area to calculate LAVI. Left ventricular dimensions were measured from parasternal views using M-mode or B-mode images if appropriate M-mode measurements were not possible to obtain. Valvular pathology was classified according to current recommendations (Vahanian et al. 2012).

Mitral annular motion measurements

Reference measurements. The acquisition is explained in Figure 1. Reference measurements of MAPSE were obtained from the apical four-chamber projection using M-mode, or anatomic M-mode from B-mode images. Reference measurements of S', e' and a' were obtained from apical four-chamber CTD recordings using the Q-analysis function in EchoPAC SWO. In the case of atrial fibrillation, no a' was measured. To quantify inter-observer agreements, another cardiologist re-analyzed the echocardiograms from 25 randomly selected patients blinded to the reference measurements.

Automatic measurements. Below, the most important concepts of the algorithm are described. For details, see Storve et al. (2016). The algorithm operates on CTD recordings (consisting of both B-mode and CTD frames) converted from DICOM (Digital Imaging and Communications in Medicine) to in-house file format.

In the first step, the algorithm uses B-mode frames to fit a deformable model with 8 control points and 75 edge detection points to the endocardial border of the left ventricle. For segmentation, the Realtime Contour Tracking Library (GE Vingmed Ultrasound) is used to encode translation, scaling, rotation and model control point positions. The shape of the model is updated with every B-mode frame. The main purpose of the model is to find the approximate location of the mitral annulus and to compensate for drift in the tracking process. The first step ends when the algorithm has analyzed 200 frames for segmentation of the left ventricle.

The algorithm narrows its search for the mitral annulus in the second step. The search is activated at the B-mode frame occurring simultaneously with the next R-wave in the electrocardiogram (ECG). A 2-D Gaussian filter is applied on the B-mode frame to eliminate speckle variations. Two 8 × 8-mm search regions extending downward from the septal and lateral sides of the model are used to detect the brightest pixel in each region, which are assumed to originate from the highly echogenic annulus.

The second step continues by activating CTD analysis. The positions of the tracked points are updated with every CTD frame by trapezoidal integration of the Doppler velocity signal. This corresponds to displacement and indicates the position change of the annulus. The principle is used to update the positions of the tracked points in the next frame. Velocity data from the tracked points, as well as their distance away from the top center of the image sector, are stored in the velocity and position buffer, respectively. At the end of the cycle (the next R-wave in the ECG), the data stored in the buffers are analyzed before repeating the second step two more times. The tracking process is restarted because integration of velocities leads to drift in the location of the tracking points over time. Because the model has already been adjusted to the left ventricle, there is no need to repeat the first step.

Measurements are acquired in the final step. For each point, MAPSE is estimated by subtracting the minimum distance from the maximum distance stored in the position buffer. To detect the peak velocities, the raw velocity signal from each tracking point in the velocity buffer is smoothed with a 1-D Gaussian filter to contain only two positive and two negative peaks. The highest of the two positive peaks is assumed to be around S', and the next two negative peaks are assumed to be around e' and a'. The algorithm then analyzes the raw velocity signal again to detect the highest absolute velocity adjacent to each peak in the smoothed signal. For all indices, septal and lateral measurements from three heart cycles are averaged.

The algorithm needs approximately six cardiac cycles to measure the mitral annular motion indices. Shorter recordings were therefore looped. The tracking process was assessed visually, and the recordings with a correctly tracked annulus (*i.e.,* when the two points were in the annular region for three consecutive cycles) were quantified. No recordings were omitted from the analyses because of failed tracking.

Statistics

Continuous variables were checked for normal distribution using the Shapiro–Wilk test and histograms. Continuous variables are reported as the mean ± standard deviation or median and first and third quartiles. Categorical variables are reported as frequencies and percentages.

The overall ability of the indices to detect LV dysfunction on the reference recordings was studied in three receiver operating characteristic (ROC) analyses. The dichotomous classification variables were based on (i) systolic and/or diastolic dysfunction, (ii) systolic dysfunction and (iii) diastolic dysfunction (yes or no). The ROC curves for MAPSE, S', e' and a' were plotted. The area under each curve (AUC) and corresponding binomial exact confidence intervals were calculated, and the AUCs were compared using the method of DeLong et al. (1988). Median and 95% confidence intervals for sensitivity, specificity, positive predictive value (PPV) and negative predictive value (NPV) for different cutoff values were calculated from 1000 bootstrap samples from the data set. The selection of cutoff values was based on the Youden index (Youden 1950). The confidence intervals were estimated using the percentage method. The agreement between two sets of measurements of the mitral annular motion indices was calculated in terms of mean difference and 95% limits of agreement.

Analyses of descriptive data and echocardiographic measurements, and random selection of cases, were done in SPSS (Version 23.0.0.0, IBM, Armonk, NY, USA). The ROC analyses were done in MedCalc (Version 12.5.0.0, MedCalc Software, Ostend, Belgium). The bootstrapping analyses were done in R (R Foundation for Statistical Computing, Vienna, Austria). For all statistical tests, a p value ≤ 0.05 was considered to indicate statistical significance.

RESULTS

Patient population

Two hundred twenty-six patients were included between September 2013 and June 2015. Four examinations were discarded from the analyses because of missing or corrupt CTD recordings. One patient withdrew the consent. This resulted in 221 patients (38% females) in the final analyses. The median age was 67 (55–75) y. Left ventricular dysfunction was identified in 60 (27%) patients by the cardiologists. Of these, 49 (82%) were classified as having systolic dysfunction and 11 (18%) as having diastolic dysfunction only. Ten medical students examined one to three patients each (20 in total). Table 1 summarizes the patients' demographic characteristics and

Table 1. Demographic characteristics and comorbidities of the 221 patients

Characteristic	Median (Q1–Q3) or n (%)		
	Normal LV function (161 patients)	Systolic dysfunction (49 patients)	Diastolic dysfunction (11 patients)
Age, y	65 (51–74)	68 (63–76)	74 (73–79)
Male gender	95 (59)	36 (73)	5 (45)
Body mass index, kg/m^2	26 (24–28)	26 (24–28)	29 (26–33)
Hypertension	85 (53)	30 (61)	9 (82)
Diabetes mellitus	19 (12)	7 (14)	2 (18)
Coronary artery disease	37 (23)	27 (55)	5 (45)
Cardiac surgery	20 (12)	12 (24)	4 (36)
Severe aortic stenosis	9 (6)	3 (6)	1 (9)
Severe mitral regurgitation	4 (2)	0	0
Pacemaker	3 (2)	5 (10)	1 (9)
Atrial fibrillation	7 (4)	14 (29)	6 (55)

LV = left ventricular; Q1 = first quartile; Q3 = third quartile.

Table 2. Echocardiographic characteristics of the 221 patients

Characteristic	Median (Q1–Q3)		
	Normal LV function (161 patients)	Systolic dysfunction (49 patients)	Diastolic dysfunction (11 patients)
Ejection fraction, %	60 (53–65)	38 (30–45)	53 (50–58)
E/*A*	1.0 (0.8–1.4)	0.9 (0.6–1.4)	2.4 (1.8–3.1)
E-wave deceleration time, ms	224 (177–285)	198 (148–252)	143 (121–171)
e′, PWTD, cm/s	8.4 (6.8–9.9)	6.6 (4.4–7.6)	7.8 (6.8–9.9)
E/*e′*, PWTD	8.4 (6.3–11.2)	12.9 (9.0–17.0)	14.4 (10.5–19.1)
IVRT, ms	92 (81–111)	101 (78–115)	63 (46–78)
S/D	1.3 (1.0–0.5)	1.2 (0.7–1.5)	0.5 (0.4–0.9)
TR peak velocity, m/s	2.5 (2.3–2.8)	2.6 (2.2–3.0)	2.9 (2.6–3.4)
LA volume index, mL/m^2	32 (27–39)	45 (36–59)	59 (43–83)
LA diameter, cm	3.9 (3.4–4.6)	4.7 (3.9–5.3)	5.1 (4.6–5.5)

A = mitral valve late inflow peak velocity; *D* = pulmonary vein diastolic flow peak velocity; *E* = mitral valve early inflow peak velocity; *e′* = mitral annular early diastolic peak velocity; IVRT = isovolumic relaxation time; LA = left atrial; LV = left ventricular; PWTD = pulsed wave tissue Doppler; Q1 = first quartile; Q3 = third quartile; *S* = pulmonary vein systolic flow peak velocity; TR = tricuspid regurgitation.

cardiovascular comorbidity, and Table 2 lists basic echocardiographic measurements from the patients with and without LV dysfunction.

Detection of left ventricular dysfunction

The ability to detect LV dysfunction with the different automatic echocardiographic indices is illustrated in Figure 2. The best predictors of systolic and/or diastolic dysfunction were MAPSE (AUC = 0.85) and *S′* (AUC = 0.83), with no significant differences between them ($p = 0.51$). The performance of *a′* (AUC = 0.78) was between those of *S′* and *e′* (AUC = 0.71) and not significantly different from them ($p > 0.21$), but *a′* had a lower AUC than MAPSE ($p = 0.04$). *e′* was the poorest predictor and was significantly different from MAPSE and *S′* ($p < 0.006$). When the indices were used to detect systolic dysfunction, MAPSE (AUC = 0.85) and *S′* (AUC = 0.83) were significantly better than *e′* (AUC = 0.76) and *a′* (AUC = 0.74) ($p < 0.03$) but were not different from each other ($p = 0.37$). Using the indices to detect isolated diastolic dysfunction provided lower predictive ability. The AUCs of MAPSE, *S′*, *e′* and *a′* were 0.67, 0.69, 0.54 and 0.78, respectively, and the only significant difference was between *e′* and *a′* ($p = 0.04$).

For the detection of systolic and/or diastolic dysfunction, the cutoff with the highest corresponding sensitivity and specificity was MAPSE ≤10 mm, with 82% sensitivity (49 cases detected, of which 42 had systolic and 7 had diastolic dysfunction), 76% specificity, 56% PPV and 92% NPV, whereas the values for *S′* ≤5.4 cm/s were nearly similar. For the detection of systolic dysfunction alone, MAPSE ≤10 mm provided 86% sensitivity (42 cases detected), 73% specificity, 48% PPV and 95% NPV. The results for detecting isolated diastolic dysfunction indicated that *a′* ≤5.3 cm/s provided 83% sensitivity (nine cases detected), 68% specificity and 99% NPV, but the PPV was low at 12%. The findings are summarized in Table 3.

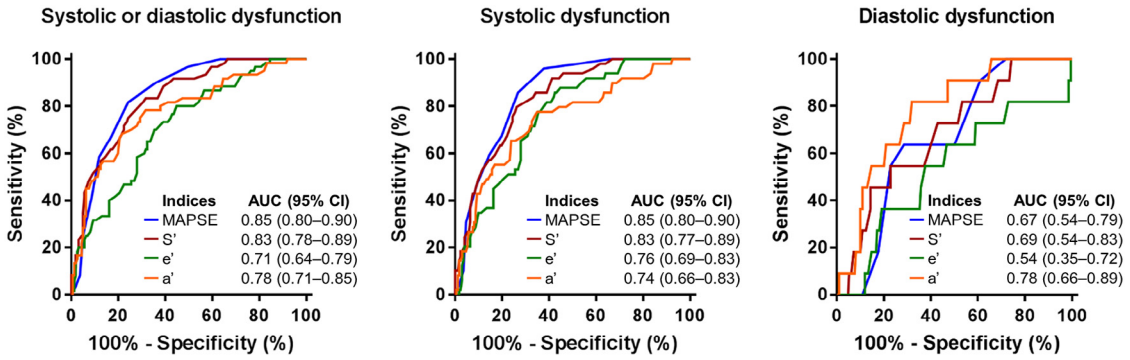

Fig. 2. Receiver operating characteristics curves for the ability of automated echocardiographic indices to detect left ventricular dysfunction in 221 study participants. Classification variable: Left ventricular dysfunction (yes or no). AUC = area under curve; CI = confidence interval; MAPSE = mitral annular plane systolic excursion; *S′* = mitral annular systolic peak velocity; *e′* = mitral annular early diastolic peak velocity; *a′* = mitral annular late diastolic peak velocity.

Table 3. Detection of left ventricular dysfunction by mitral annular motion indices

Index	Cutoff	Median (95% CI) Sensitivity (%)	Specificity (%)	PPV (%)	NPV (%)
Systolic or diastolic dysfunction (60/221 patients)					
MAPSE	≤10 mm	82 (72–90)	76 (69–82)	56 (46–66)	92 (87–96)
S′	≤5.4 cm/s	83 (74–92)	68 (61–75)	49 (41–60)	92 (86–96)
e′	≤5.6 cm/s	70 (58–81)	64 (57–71)	42 (33–52)	85 (79–91)
a′	≤6.1 cm/s	79 (67–89)	68 (62–76)	48 (38–58)	89 (84–95)
Systolic dysfunction (49/221 patients)					
MAPSE	≤10 mm	86 (75–96)	73 (66–79)	48 (38–58)	95 (90–98)
S′	≤5.1 cm/s	79 (68–91)	74 (67–80)	46 (35–57)	93 (88–97)
e′	≤6.1 cm/s	86 (76–95)	57 (50–65)	36 (28–45)	94 (88–98)
a′	≤6.1 cm/s	78 (66–89)	65 (58–72)	39 (30–48)	91 (86–96)
Diastolic dysfunction (11/221 patients)					
MAPSE	≤9 mm	64 (33–92)	71 (66–78)	10 (3–18)	97 (95–99)
S′	≤3.9 cm/s	44 (13–75)	86 (81–90)	14 (3–27)	97 (94–99)
e′	≤9.1 cm/s	92 (71–100)	12 (8–16)	5 (3–9)	96 (88–100)
a′	≤5.3 cm/s	83 (56–100)	68 (61–75)	12 (5–19)	99 (96–100)

a′ = mitral annular late diastolic peak velocity; CI = confidence interval; *e′* = mitral annular early diastolic peak velocity; MAPSE = mitral annular plane systolic excursion; NPV = negative predictive value; PPV = positive predictive value; *S′* = mitral annular systolic peak velocity.

Comparison of mitral annular motion measurements

In general, the agreement between measurements was highest for the systolic indices. When the algorithm was run on the 221 reference recordings, the mean difference compared with manual reference measurements was –0.2 ± 2.1 mm for MAPSE and –0.1 ± 0.9 cm/s for *S′*. In the inter-observer analysis, the mean difference between the cardiologist's 25 extra measurements and the reference was 1.0 ± 1.6 mm for MAPSE and –0.1 ± 0.5 cm/s for *S′*. For the 20 student recordings, the mean differences from the reference for these two indices were –0.8 ± 3.2 mm and –0.1 ± 1.6 cm/s. The results are elaborated in Table 4.

In 190 (86%) of the reference recordings and in 15 (75%) of the student recordings, the algorithm tracked the mitral annulus correctly, assessed by visual inspection. On the reference recordings from the patients examined by the students, the tracking was successful in 16 (80%) of the cases, and 17 (85%) of the tracking results from reference and student recordings were identical.

Table 4. Comparison of measurements of mitral annular motion indices

Cardiologist on reference recordings versus reference measurements					
Index	No. of pairs	Cardiologist (mean ± SD)	Reference (mean ± SD)	Mean (diff ± SD)	95% LA
MAPSE, mm	25	11.9 ± 3.1	10.9 ± 2.7	1.0 ± 1.6	–2.2 to 4.1
S′, cm/s	25	5.4 ± 1.5	5.5 ± 1.4	–0.1 ± 0.5	–1.1 to 0.9
e′, cm/s	25	5.7 ± 2.2	5.4 ± 2.1	0.3 ± 1.1	–2.0 to 2.7
a′, cm/s	21	7.5 ± 1.9	7.3 ± 1.8	0.2 ± 0.4	–0.7 to 1.1
Algorithm on reference recordings versus reference measurements					
Index	No. of pairs	Algorithm (mean ± SD)	Reference (mean ± SD)	Mean (diff ± SD)	95% LA
MAPSE, mm	221	11.2 ± 3.4	11.5 ± 2.9	–0.2 ± 2.1	–4.3 to 3.8
S′, cm/s	221	5.6 ± 1.7	5.7 ± 1.7	–0.1 ± 0.9	–1.7 to 1.7
e′, cm/s	221	6.2 ± 2.6	5.8 ± 2.3	0.4 ± 1.4	–2.7 to 3.2
a′, cm/s	194	6.4 ± 2.5	6.9 ± 2.0	–0.1 ± 1.4	–2.8 to 2.6
Algorithm on student recordings versus reference measurements					
Index	No. of pairs	Algorithm (mean ± SD)	Reference (mean ± SD)	Mean (diff ± SD)	95% LA
MAPSE, mm	20	11.7 ± 3.4	12.5 ± 2.2	–0.8 ± 3.2	–7.1 to 5.5
S′, cm/s	20	6.1 ± 1.8	6.1 ± 1.6	–0.1 ± 1.6	–3.3 to 3.1
e′, cm/s	20	6.7 ± 2.3	6.7 ± 2.7	–0.1 ± 1.9	–3.9 to 3.7
a′, cm/s	20	6.2 ± 2.2	6.9 ± 1.9	–0.7 ± 1.8	–4.2 to 2.9

a′ = mitral annular late diastolic peak velocity; diff = difference; *e′* = mitral annular early diastolic peak velocity; LA = limits of agreement; MAPSE = mitral annular plane systolic excursion; *S′* = mitral annular systolic peak velocity; SD = standard deviation.

DISCUSSION

We found that the automatic analyses of systolic mitral annular motion indices detected LV dysfunction with a high sensitivity, negative predictive value and adequate specificity. It was more difficult to detect diastolic dysfunction than systolic dysfunction. Reliance on either MAPSE or S' measurements seems to be the most useful solution.

As reported previously by others, LV long-axis indices are sensitive enough to detect both subclinical LV dysfunction and change in LV performance (Dalen et al. 2011; Thavendiranathan et al. 2014; Thorstensen et al. 2011). The lower normal limit of MAPSE measured manually by M-mode in healthy adults has been reported to be around 10–12 mm (Elnoamany and Abdelhameed 2006; Hoglund et al. 1988; Mondillo et al. 2006), and the same values have been proposed as cutoff values for the detection of systolic dysfunction (Alam et al. 1992; Elnoamany and Abdelhameed 2006). In our material, the largest number of patients in whom LV dysfunction was detected was seen when an automatically measured MAPSE ≤10 mm was the cut-off value for detection of systolic and/or diastolic dysfunction. Considering the two entities of LV dysfunction separately, the best results were seen for detection of systolic dysfunction. Several studies on detection of LV dysfunction report better results, but such data should be interpreted in light of patient populations, disease definitions and imaging modalities. Alam et al. (1992) found that MAPSE <10 mm measured manually by M-mode detected systolic dysfunction (EF <55%) with 92% sensitivity and 87% specificity among patients with coronary artery disease and healthy controls. The lower specificity in our study might be a result of the mixed patient population including patients with diastolic dysfunction. There was also a high prevalence of diseases known to impair LV long-axis function—for example, hypertension, aortic stenosis and diabetes (Hu et al. 2013)—among the patients classified with normal LV function (*i.e.,* EF ≥50% and without signs of elevated filling pressure).

From a large study of normal ranges, 4.6 cm/s could represent a lower reference value for S' (Dalen et al. 2010). Using this as the cutoff for detection of systolic dysfunction in our material provided lower sensitivity (63%), but higher specificity (80%) compared with S' ≤5.4 cm/s. With manual CTD and a cutoff for S' <4.4 cm/s, Yu et al. (2002) reported a sensitivity of 92% for systolic dysfunction (EF <50%) and a sensitivity of 52% for mild or moderate diastolic dysfunction. Other studies have reported that a reduced S' measured manually by PW tissue Doppler predicts systolic dysfunction (EF <50%) with a sensitivity from 80% to 94% and a specificity from 89% to 93% (Elnoamany and Abdelhameed 2006; Vinereanu et al. 2002). In a sample consisting only of patients with diastolic dysfunction (EF >45%) and healthy controls, Garcia et al. (2006) found that S' measured manually by PW tissue Doppler detected the abnormal cases with a sensitivity of 97% and a specificity of 73%. By comparing only patients with diastolic dysfunction and those without any cardiovascular disease, we obtained a similar result (data not shown), but this approach is misleading because patients with systolic function will be part of a real-world population.

e' is a well-established index for assessment of diastolic function (Nagueh et al. 2016). The e'/a' ratio has been studied as a potential index of diastolic dysfunction, but reports are inconsistent (Kasner et al. 2007; Lee et al. 2012). One of its weaknesses is similar to the E/A ratio: The e'/a' ratio has a U-shaped distribution in the continuum between normal and severely impaired diastolic (Sohn et al. 1997). Because patients with systolic dysfunction were overrepresented compared with patients with diastolic dysfunction in this study, it is not surprising that the systolic indices MAPSE and S' outperformed the diastolic indices e' and a'. Combining the mitral annular motion indices in a logistic regression model for classification of LV function is an interesting approach, but explorative analyses in our material indicate no gain in predictive ability at the expense of a more complex model (data not shown).

The definition used for classification of LV diastolic dysfunction was not identical to current guidelines (Nagueh et al. 2016). Diastolic dysfunction was defined as EF ≥50% and signs of elevated filling pressure. High filling pressure is seen in severe cases of diastolic dysfunction, whereas an EF <30 is considered as severe systolic dysfunction. We did not test the algorithm's ability to detect milder states of diastolic dysfunction and this may have influenced the performance of the different echocardiographic indices. Only LV dysfunction was targeted in this study. Right ventricular dysfunction and valvular disease can also cause heart failure, but the indices measured by the algorithm are not suitable for detecting such conditions.

Mitral annular motion measurements should be based on at least three consecutive cardiac cycles (Nagueh et al. 2009). In 45% of the reference CTD recordings, only one or two cardiac cycles were recorded. Several studies have concluded that reference values of mitral annular motion measurements should be age and gender specific (Dalen et al. 2010; Nikitin et al. 2003). By increasing age, e' is reduced more than MAPSE and S', while a' increases with age. Gender differences are not as distinct. We did not use age- or gender-specific cut-off values. Adjusting for age and sex could easily be implemented in future scanners.

During one cardiac cycle, the algorithm is programmed to detect two negative peak velocities, which correspond to e' and a'. In the case of atrial fibrillation, the a' wave will not actually be present, and the

algorithm will fail in measuring the diastolic velocities. This makes e' and a' measurements less reliable. Relying on MAPSE and S', which are both measured during systole, excludes this problem. Because there is no inherent need for an electrocardiogram for the algorithm to work (Storve et al. 2016), automatic comparisons of heart cycle durations could be used to detect atrial fibrillation and deactivate a' measurements.

The automatic measurements from the reference recordings had a nearly similar agreement with the reference as the expert inter-observer agreement, even though the automatic measurements were partly obtained from different recordings, and also by using a different method. The results are comparable to the findings of de Knegt et al. (2014), who studied inter-observer agreement between experts for mitral annular motion measurements. Measurements from student recordings had a lower agreement with the reference. This is probably mostly due to the short training period of the students, followed by the aforementioned factors. With more practice in image acquisition, we expect increased measurement quality. A limitation of this study is that the agreement between the measurements of the different observers and modalities have not been studied under identical conditions. When measurements are repeated on the same recordings, higher agreement can be expected when the measurements are acquired from different recordings.

CONCLUSIONS

Automatic measurements of mitral annular motion were helpful in the detection of LV dysfunction. The best indices for detection of LV dysfunction in this study were MAPSE and S', but they should be evaluated in the context of other variables such as valvular function and should be studied in other populations.

REFERENCES

Alam M, Hoglund C, Thorstrand C, Hellekant C. Haemodynamic significance of the atrioventricular plane displacement in patients with coronary artery disease. Eur Heart J 1992;13:194–200.

Atherton JJ. Screening for left ventricular systolic dysfunction: Is imaging a solution? JACC Cardiovasc Imaging 2010;3:421–428.

Bruch C, Gradaus R, Gunia S, Breithardt G, Wichter T. Doppler tissue analysis of mitral annular velocities: Evidence for systolic abnormalities in patients with diastolic heart failure. J Am Soc Echocardiogr 2003;16:1031–1036.

de Knegt MC, Biering-Sorensen T, Sogaard P, Sivertsen J, Jensen JS, Mogelvang R. Concordance and reproducibility between M-mode, tissue Doppler imaging, and two-dimensional strain imaging in the assessment of mitral annular displacement and velocity in patients with various heart conditions. Eur Heart J Cardiovasc Imaging 2014;15:62–69.

Dalen H, Thorstensen A, Romundstad PR, Aase SA, Stoylen A, Vatten LJ. Cardiovascular risk factors and systolic and diastolic cardiac function: A tissue Doppler and speckle tracking echocardiographic study. J Am Soc Echocardiogr 2011;24:322–332.

Dalen H, Thorstensen A, Vatten LJ, Aase SA, Stoylen A. Reference values and distribution of conventional echocardiographic Doppler measures and longitudinal tissue Doppler velocities in a population free from cardiovascular disease. Circ Cardiovasc Imaging 2010;3:614–622.

DeLong ER, DeLong DM, Clarke-Pearson DL. Comparing the areas under two or more correlated receiver operating characteristic curvesa: Nonparametric approach. Biometrics 1988;44:837–845.

Elnoamany MF, Abdelhameed AK. Mitral annular motion as a surrogate for left ventricular function: Correlation with brain natriuretic peptide levels. Eur J Echocardiogr 2006;7:187–198.

Garcia EH, Perna ER, Farias EF, Obregon RO, Macin SM, Parras JI, Aguero MA, Moratorio DA, Pitzus AE, Tassano EA, Rodriguez L. Reduced systolic performance by tissue Doppler in patients with preserved and abnormal ejection fraction: New insights in chronic heart failure. Int J Cardiol 2006;108:181–188.

Hoglund C, Alam M, Thorstrand C. Atrioventricular valve plane displacement in healthy persons: An echocardiographic study. Acta Med Scand 1988;224:557–562.

Hu K, Liu D, Herrmann S, Niemann M, Gaudron PD, Voelker W, Ertl G, Bijnens B, Weidemann F. Clinical implication of mitral annular plane systolic excursion for patients with cardiovascular disease. Eur Heart J Cardiovasc Imaging 2013;14:205–212.

Kadappu KK, Thomas L. Tissue Doppler imaging in echocardiography: Value and limitations. Heart Lung Circ 2015;24:224–233.

Kasner M, Westermann D, Steendijk P, Gaub R, Wilkenshoff U, Weitmann K, Hoffmann W, Poller W, Schultheiss HP, Pauschinger M, Tschope C. Utility of Doppler echocardiography and tissue Doppler imaging in the estimation of diastolic function in heart failure with normal ejection fraction: A comparative Doppler-conductance catheterization study. Circulation 2007;116:637–647.

Lee CH, Hung KC, Chang SH, Lin FC, Hsieh MJ, Chen CC, Chu CM, Hsieh IC, Wen MS, Wu D. Reversible left ventricular diastolic dysfunction on Doppler tissue imaging predicts a more favorable prognosis in chronic heart failure. Circ J 2012;76:1145–1150.

McMurray JJ, Adamopoulos S, Anker SD, Auricchio A, Bohm M, Dickstein K, Falk V, Filippatos G, Fonseca C, Gomez-Sanchez MA, Jaarsma T, Kober L, Lip GY, Maggioni AP, Parkhomenko A, Pieske BM, Popescu BA, Ronnevik PK, Rutten FH, Schwitter J, Seferovic P, Stepinska J, Trindade PT, Voors AA, Zannad F, Zeiher A, Bax JJ, Baumgartner H, Ceconi C, Dean V, Deaton C, Fagard R, Funck-Brentano C, Hasdai D, Hoes A, Kirchhof P, Knuuti J, Kolh P, McDonagh T, Moulin C, Popescu BA, Reiner Z, Sechtem U, Sirnes PA, Tendera M, Torbicki A, Vahanian A, Windecker S, McDonagh T, Sechtem U, Bonet LA, Avraamides P, Ben Lamin HA, Brignole M, Coca A, Cowburn P, Dargie H, Elliott P, Flachskampf FA, Guida GF, Hardman S, Iung B, Merkely B, Mueller C, Nanas JN, Nielsen OW, Orn S, Parissis JT, Ponikowski P. ESC guidelines for the diagnosis and treatment of acute and chronic heart failure 2012: The Task Force for the Diagnosis and Treatment of Acute and Chronic Heart Failure 2012 of the European Society of Cardiology. Developed in collaboration with the Heart Failure Association (HFA) of the ESC. Eur J Heart Fail 2012;14:803–869.

Mondillo S, Galderisi M, Ballo P, Marino PN. Left ventricular systolic longitudinal function: Comparison among simple M-mode, pulsed, and M-mode color tissue Doppler of mitral annulus in healthy individuals. J Am Soc Echocardiogr 2006;19:1085–1091.

Nagueh SF, Appleton CP, Gillebert TC, Marino PN, Oh JK, Smiseth OA, Waggoner AD, Flachskampf FA, Pellikka PA, Evangelisa A. Recommendations for the evaluation of left ventricular diastolic function by echocardiography. Eur J Echocardiogr 2009;10:165–193.

Nagueh SF, Smiseth OA, Appleton CP, Byrd BF, 3rd, Dokainish H, Edvardsen T, Flachskampf FA, Gillebert TC, Klein AL, Lancellotti P, Marino P, Oh JK, Popescu BA, Waggoner AD. Recommendations for the evaluation of left ventricular diastolic function by echocardiography: An update from the american society of echocardiography and the European Association of Cardiovascular Imaging. J Am Soc Echocardiogr 2016;29:277–314.

Nikitin NP, Witte KK, Thackray SD, de Silva R, Clark AL, Cleland JG. Longitudinal ventricular function: Normal values of atrioventricular annular and myocardial velocities measured with quantitative

two-dimensional color Doppler tissue imaging. J Am Soc Echocardiogr 2003;16:906–921.

Ponikowski P, Voors AA, Anker SD, Bueno H, Cleland JG, Coats AJ, Falk V, Gonzalez-Juanatey JR, Harjola VP, Jankowska EA, Jessup M, Linde C, Nihoyannopoulos P, Parissis JT, Pieske B, Riley JP, Rosano GM, Ruilope LM, Ruschitzka F, Rutten FH, van der Meer P. 2016 ESC Guidelines for the diagnosis and treatment of acute and chronic heart failure: The Task Force for the diagnosis and treatment of acute and chronic heart failure of the European Society of Cardiology (ESC). Developed with the special contribution of the Heart Failure Association (HFA) of the ESC. Eur J Heart Fail 2016; 18:891–975.

Sohn DW, Chai IH, Lee DJ, Kim HC, Kim HS, Oh BH, Lee MM, Park YB, Choi YS, Seo JD, Lee YW. Assessment of mitral annulus velocity by Doppler tissue imaging in the evaluation of left ventricular diastolic function. J Am Coll Cardiol 1997;30:474–480.

Storve S, Grue JF, Samstad S, Dalen H, Haugen BO, Torp H. Realtime automatic assessment of cardiac function in echocardiography. IEEE Trans Ultrason Ferroelectr Freq Control 2016;63:358–368.

Thavendiranathan P, Poulin F, Lim KD, Plana JC, Woo A, Marwick TH. Use of myocardial strain imaging by echocardiography for the early detection of cardiotoxicity in patients during and after cancer chemotherapya: Systematic review. J Am Coll Cardiol 2014;63: 2751–2768.

Thorstensen A, Dalen H, Amundsen BH, Stoylen A. Peak systolic velocity indices are more sensitive than end-systolic indices in detecting contraction changes assessed by echocardiography in young healthy humans. Eur J Echocardiogr 2011;12:924–930.

Vahanian A, Alfieri O, Andreotti F, Antunes MJ, Baron-Esquivias G, Baumgartner H, Borger MA, Carrel TP, De Bonis M, Evangelista A, Falk V, Lung B, Lancellotti P, Pierard L, Price S, Schafers HJ, Schuler G, Stepinska J, Swedberg K, Takkenberg J, Von Oppell UO, Windecker S, Zamorano JL, Zembala M. Guidelines on the management of valvular heart disease (version 2012): The Joint Task Force on the Management of Valvular Heart Disease of the European Society of Cardiology (ESC) and the European Association for Cardio-Thoracic Surgery (EACTS). Eur J Cardiothorac Surg 2012;42:S1–S44.

Vinereanu D, Khokhar A, Tweddel AC, Cinteza M, Fraser AG. Estimation of global left ventricular function from the velocity of longitudinal shortening. Echocardiography 2002;19:177–185.

Yip G, Wang M, Zhang Y, Fung JW, Ho PY, Sanderson JE. Left ventricular long axis function in diastolic heart failure is reduced in both diastole and systole: Time for a redefinition? Heart 2002;87:121–125.

Youden WJ. Index for rating diagnostic tests. Cancer 1950;3:32–35.

Yu CM, Lin H, Yang H, Kong SL, Zhang Q, Lee SW. Progression of systolic abnormalities in patients with "isolated" diastolic heart failure and diastolic dysfunction. Circulation 2002;105:1195–1201.